LA-UR-91-1837

TITLE   MEASUREMENT OF MOLYBDENUM MIRROR REFLECTIVITIES

AUTHOR(S)   R.L. Blake, J.C. Davis, P.P. Gong, D. E. Graessle,
and W. Ruderman

SUBMITTED TO   Society of Photo-Optical Instrumentation Engineers
SPIE Proceedings
1000 20th. Street
P.O. Box 10
Bellingham, WA 98227-0010

Los Alamos

Los Alamos National Laboratory
Los Alamos, New Mexico 87545

MASTER

Measurement of molybdenum mirror reflectivities

R. L. Blake and J. C. Davis

Los Alamos National Laboratory
MS D410, Los Alamos, NM 87545

P. P. Gong

EG&G/EM Inc., MS F4
P. O. Box 1912, Las Vegas, NV 89125

D. E. Graessle

Harvard-Smithsonian Astrophysical Observatory
60 Garden St., Cambridge, MA 02138

W. Rudderman

INRAD, Inc.
181 Legrand Ave., Northvale, NJ 07647

ABSTRACT

The reflectivity versus angle for a variety of molybdenum mirrors has been measured for both hard and soft X-Rays in an attempt to deduce any variation in performance between single crystal, polycrystalline, and evaporated mirrors. A fitting technique has been used to arrive at the roughness of the mirrors. An approach to utilize such measurements to characterize mirrors and derive low energy optical constants for many elements is outlined.

1 INTRODUCTION

Mirror reflectivities in the XUV and X-Ray ranges are important for several reasons. There is a pressing need for direct calibrations of mirrors in space borne x-ray telescopes.[1] Secondly, one can determine contamination layers and densities of thin films on optical surfaces from x-ray reflectivity measurements.[2] Third, surface roughness can be modeled via reflectivity versus angle of incidence measurements.[3-5] This is important because roughness plays a critical role in the qua ty of x-ray imaging optics. Finally, if one can adequately control or measure the density and roughness, it becomes possible to derive the optical constants[6] of many materials in the XUV range from reflectivity data.[7,8]

This paper outlines and gives preliminary results of a program aimed at contributions to each of the above areas. We will exploit the versatility of an existing precision vacuum reflectometer[9] and the availability of synchrotron beams tunable over the range from 30 eV to 30 keV.[10,11] Measurements in the 5 15 keV range, where optical constants are accurately known, will permit determinations of density and roughness parameters of many samples. Additional measurements at XUV energies from the same samples will permit us to extract information a bout contamination layers and the XUV optical constants, which are not well known.

Optical constants f_1 and f_2, or alternatively δ and β, can be derived by fitting to reflectivity data. The measured data are absolute reflectivity as a function of angle at a fixed energy. The advantage of this formulation is that both the real and imaginary parts of the complex index of refraction are directly obtained and it is possible to avoid doing any Kramers-Kronig analysis which is required to obtain δ or f_1 from absorption data.

This method of obtaining optical constants is most useful at lower energi s where transmission measurements would require the use of extremely thin films which are difficult to handle and characterize. Good optical constants are needed for calculating theoretical responses of various optics for the XUV region. For example, optical constants for Molybdenum below 200 eV are derived from either a single source or from two or more sources which do not agree.[12,13] If Mo is to be used as an optic in the XUV region its optical constants must be measured and its performance characterized. A similar problem exists for most other useful materials.

We have confined this paper to Mo results because some work has been done in the XUV region[7] and because samples were available in bulk forms (single crystal and polycrystalline) as well as evaporated and sputtered samples on optical substrates. The method described is of general applicability.

2 EXPERIMENTAL PROCEDURE AND APPARATUS

Reflectivity data were taken on the X8C[11] and U3C[10] beamlines at the National Synchrotron Light Source located at Brookhaven National Laboratory. The energy ranges available are 5 to 20 keV for X8C and 30 to 1200 eV for U3C. Further measurements are planned for X8A, which covers the energy range between X8C and U3C. A fourth beamline, U3A, supplemental to U3C and covering the same or expanded energy range, will be used in future work.[14] The instrument used was a single crystal spectrometer, used as a reflectometer, which functions both in air and in vacuum.[9] In both cases a vertical slit was used in order to insure that the entire beam was intercepted by the mirror. The width of this slit placed a lower limit on the minimum angle at which the entire beam was intercepted.

Our Measurement approach is an adaptation of the Bond method[15] for accurate crystal lattice constant determination. Figure 1 illustrates the method. Radiation incident through the collimator falls upon the crystal in the
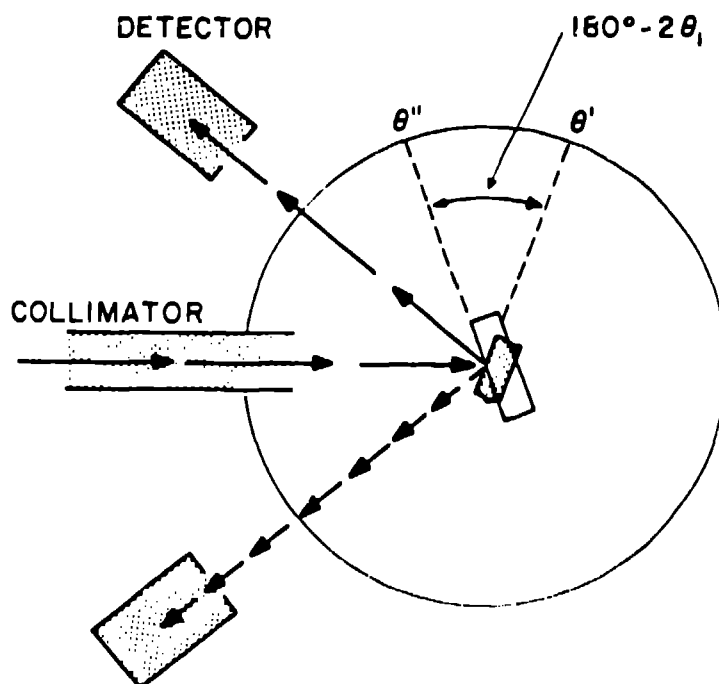

Figure 1: Schematic of the measuring technique.

shaded position. By scanning the crystal through angles θ and the detector through angles 2θ one generates a line profile with a peak at θ'. Next the crystal is moved to the unshaded position to reflect the beam to the opposite side of the incident beam plane. A similar angular scan over a small range leads to another profile with a peak at θ''. If an nth order reflection is being measured, the true angle θ_n for the peak follows from the geometry of Bragg reflection, $\theta_n = 90° - (\theta'' - \theta')/2$. The rotary table zero angle is irrelevant because only the difference $\theta'' - \theta'$ enters in the determination of θ_n. All known sources of error and alignment technique are discussed by Blake[16] and Thomsen.[17] A key feature is that the entire beam passed by the collimator is intercepted by the crystal (or mirror) and by the detector., Then only modest accuracy is demanded on the detector angle · so that variations in detector sensitivity over the entrance area are negligible. Also, the incident beam flux I_0 can be measured directly by simply lifting the sample (crystal or mirror) out of the beam when the detector is brought to nominal zero angle. Our sample holders are designed for removal and replacement with an angle uncertainty not exceeding 1″. The turntables have a calibration accuracy of 2″, correctable to 1″.

When measuring mirrors rather than crystals there is no sharply defined Bragg peak. Rather there is a critical angle cutoff and a gradual decline towards increased glancing angles. At high energies ≈ 10 keV the critical angle cutoff is ≈ 5 mrad or less than 30′. High accuracy fitting of the profile requires careful measurement of the true reflectivity on each side of the incident beam plane. A simple program called SWAPO does this, it is iterated

until the profiles coincide on a plot. An accuracy of $10^{\prime\prime}$ has been obtained with our preliminary data, with an expected potential accuracy of approximately $1^{\prime\prime}$. Unfortunately the process must be repeated occasionally, since synchrotron orbits move slightly in unpredictable ways.

Data reported here were measured with Xenon filled proportional counters from 5 to 12 keV and with X-Ray diodes from 100 to 1000 eV. The former required slits of $\approx 10\mu m \times 10\mu m$ to keep the count rate below 10^4 cps. The latter were limited by scattered light and harmonics from the monochromator.

The automation and data acquisition software for the beamline and spectrometer is written for the DEC Microvax. Motors are controlled by DSP E500 modules residing in a CAMAC crate. Counting is done by Kinetics 3610 or 3615 scaler modules. Timing is done with a DSP RTC018 real time clock.

On X8C I_0 was monitored by an ion chamber in the direct beam and a proportional counter measuring air scattered radiation, both detectors being located upstream of the slit just before the mirror (In the future the they must be located downstream of the slit for accurate results). The ion chamber's current output was converted to a frequency and this was measured by the 3615. Continuous monitoring of I_0 was necessary since the intensity coming from the synchrotron fluctuates with time. At the beginning and end of each run the sample was lifted out and the normalization constant (counts for reflection detector/counts for scattering detector) was measured.

The proportional counters for X8C were sealed rather than flow counters. The output of each was fed into a preamp, amplifier, and then into a pair of SCA's. The windows on the SCA were set such that the primary radiation was counted on one channel and the higher order components were counted on another. The output of each SCA was counted by the 3615, which was in turn read by the Microvax. This gave a measure of harmonic contamination and improved harmonic rejection over that achieved via detuning of the monochromator alone.

On U3C a mesh monitor was used to normalize all measurements and a calibrated NBS diode was used for reflection and incident beam (I_0) measurements. The sample was again lifted out at the beginning and end of each run. Electrometers were used for each detector, fed into a voltage to frequency converter, and then into the 3615 which was read by the Microvax.

On U3C the reflectivity versus angle scans were done by hand, while the reflectivity versus energy at fixed angle was automated. The latter exhibits an energy cutoff (see figure 2). These preliminary data are limited by scattered light, higher order harmonics, and geometric idiosyncrasies.

It seemed prudent to start our program with measurements on X8C at energies of $\approx 5 - 10$ keV and with bulk density samples. Then density and optical constants are known well enough and only the surface roughness needs evaluation.

3 MODEL

Surface roughness reduces specular reflectivity from an X-Ray mirror. In analyzing our X8C data we have used a model developed by D. G. Stearns.[4] If we assume that the averaged surface density may be modeled as a smear of profile $p(z)\rho$ and its derivative $w(z)\rho$, the reflectivity is given by

$$R = R_F \tilde{w}(-2k),\tag{1}$$

where R_F is the Fresnel reflectivity and $\tilde{w}$ is the Fourier transform of w. For $p(z)$ we have chosen the error function:

$$p(z) = \frac{1}{\sqrt{\pi}} \int_{-\infty}^{z} \exp(-t^2/2\sigma^2)\, dt,\tag{2}$$

where σ represents the transition thickness and is defined as

$$\sigma^2 = \int z^2 w(z)dz.\tag{3}$$

As a result, the equation for the reflectivity (for each polarization) is

$$R_{\parallel}(\theta) = \left| \frac{\sin\theta - \gamma}{\sin\theta + \gamma} \right|^2 e^{-(\cdots)^2},\tag{4}$$

and

$$R_{\perp}(\theta) = \left| \frac{n^2\sin\theta - \gamma}{n^2\sin\theta + \gamma} \right|^2 e^{-(\cdots)^2},\tag{5}$$
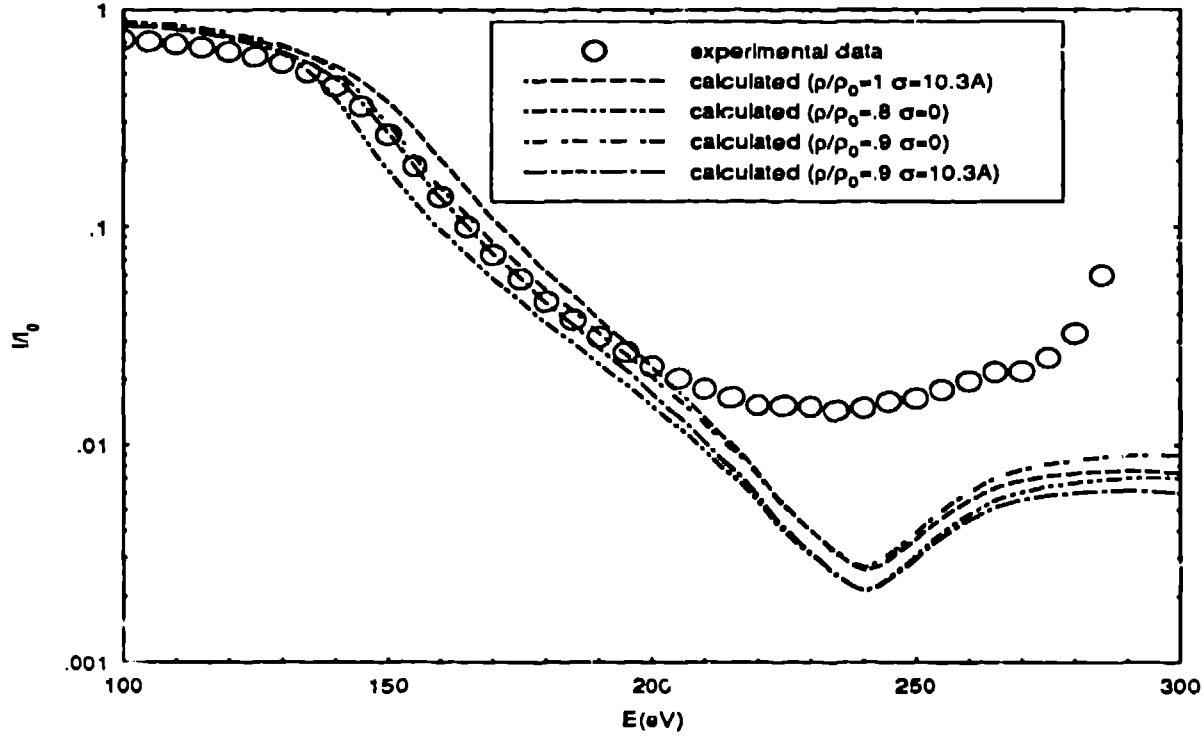
Figure 2: U3C energy scan with $\theta = 204\,$mrad.

where $n = 1 - \delta - i\beta$ and $\gamma = \sqrt{n^2 + \sin^2\theta - 1}$. Polarization effects are negligible in the angle range of interest and so the average of equations (4) and (5) was used to fit the experimental data.

It must be remarked that since (1) was derived in the context of first order scattering theory it is valid only in the region above the critical angle, $\theta_c \approx \sqrt{2\delta}$ (for Mo this ranges from 12.25 mrad at 5 kev to 5.5 mrad at 11 keV). Near the critical angle the model reduces the reflectivity too much. Hence when fitting for δ, data below the critical angle must be ignored.

4 REDUCTION OF EXPERIMENTAL DATA

The experimental reflectivity was calculated from:

$$ R = \frac{I}{I_0} = \frac{(M - B)}{S}\frac{S_N}{M_N}, \tag{6} $$

where M is the counts on the mirror detector and S the counts on the scattering detector during the reflected beam measurement, M_N the counts on the mirror detector and S_N the counts on the scattering detector with the mirror removed during incident beam measurements, and B is the background counts (≈ 6 cps with the Xenon sealed proportional counter). The statistical error in R is given by

$$ \sigma_R = R\sqrt{\left(\frac{\sqrt{\sigma_M^2 + \sigma_B^2}}{M - B}\right)^2 + \left(\frac{\sigma_S}{S}\right)^2 + \left(\frac{\sigma_{M_N}}{M_N}\right)^2 + \left(\frac{\sigma_{S_N}}{S_N}\right)^2}, \tag{7} $$

This equation implicitly assumes that the error in a given counter is not correlated with the error in any other counter. The error, σ, for each individual measurement (S, M) is assumed to be $\sqrt{N}$ where N is the number of counts. So this reduces to

$$ \sigma_R = R\sqrt{\frac{M + \sigma_B^2}{(M - B)^2} + \frac{1}{S} + \left(\frac{\sigma_{M_N}}{M_N}\right)^2 + \left(\frac{\sigma_{S_N}}{S_N}\right)^2}. \tag{8} $$

The dominant error present in our data was from low count rates in the tails of the reflectivity curve. Above roughly 12 mrad the background dominated the signal and resulted in 50% to 100% errors.

Systematic errors were recognized and not fully compensated in these preliminary data. At small angles R is too small because deadtime corrections were not made. More importantly, the mirror mounts caused interference at small angles. Otherwise, our slit system would have permitted accurate R values down to $\approx$ 1mrad. Occasional oscillations of up to 10% amplitude were observed and not removed, nor yet understood.

The experimental data were fit by minimizing the χ^2 error measure,

$$\chi^2 = \sum_{i=1}^{N} \frac{(R_{exp,i} - R(\theta_i))^2}{\sigma_{R_i}^2} .$$

(9)

The error function was minimized with the Levenberg-Marquardt algorithm.[18] Fits to σ for a single crystal molybdenum sample at energies from 5 to 11 keV are shown in figure 3. The δ and β values were taken from Henke,

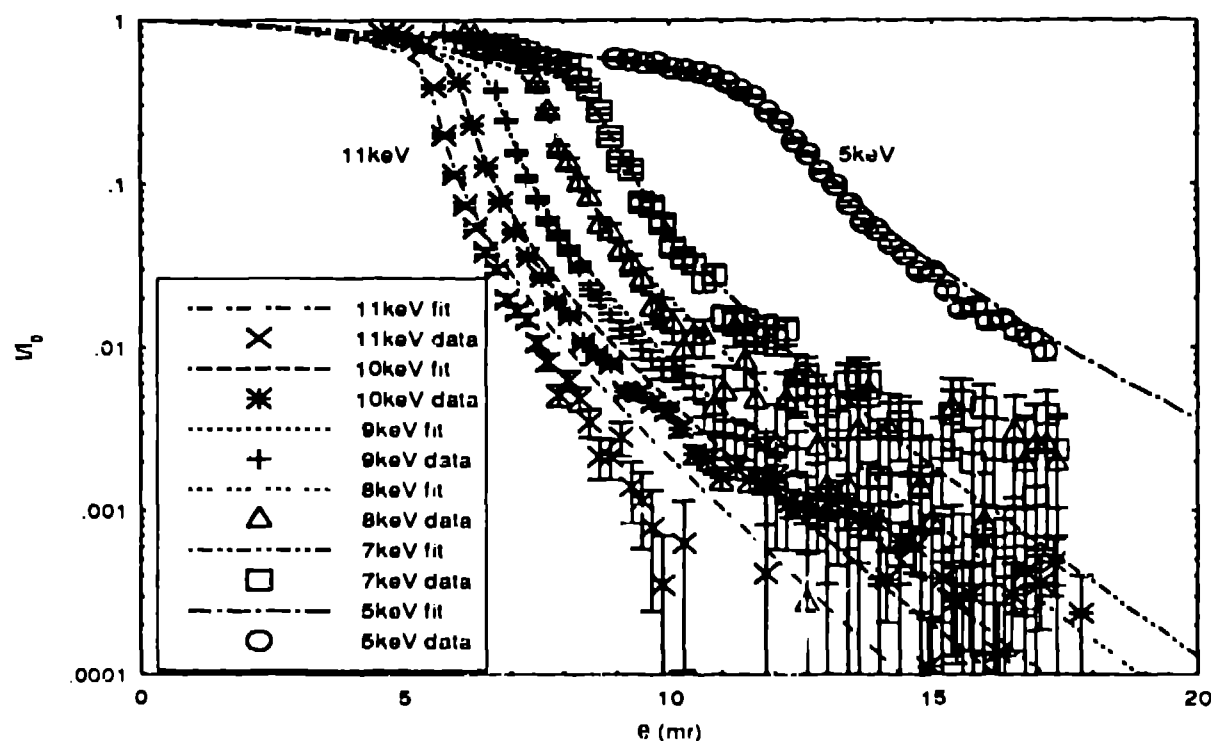**Single Crystal Molybdenum σ fits for (5,7,8,9,10,11) keV**

Figure 3: Single crystal molybdenum angle scans at energies from 5 to 11 keV.

et. al [6] and are accurate values since at higher energy the optical constants are well characterized.

A few comments can be made about data shown in figure 3. When using higher energy reflectivity curves to obtain density and roughness it should be sufficient to choose one or two energies at which to make very careful measurements versus glancing angle. Good results on roughness require good accuracy in the region above the critical angle and a dynamic range of about 10^5. Our roughness model is only valid above the critical angle. Therefore, the "poor fit" below the critical angle should be ignored. These data on single crystal Mo have no ambiguity regarding density or optical constants. Hence, one can concentrate on the roughness parameter. This is also the case for polycrystalline Mo.

Figures 4 and 5 also show superposed 10 keV reflectivity curves for single crystal and polycrystalline Mo, respectively. Figure 4 includes five curves, four from the positive side of the incident beam and one from the negative side. The positive side data include measurements when the mirror is rotated 180° about an axis normal to the mirror surface. Clearly the goodness of fit for roughness and for density or optical constants depends on the accuracy of the zero correction and on invariance under this rotation.
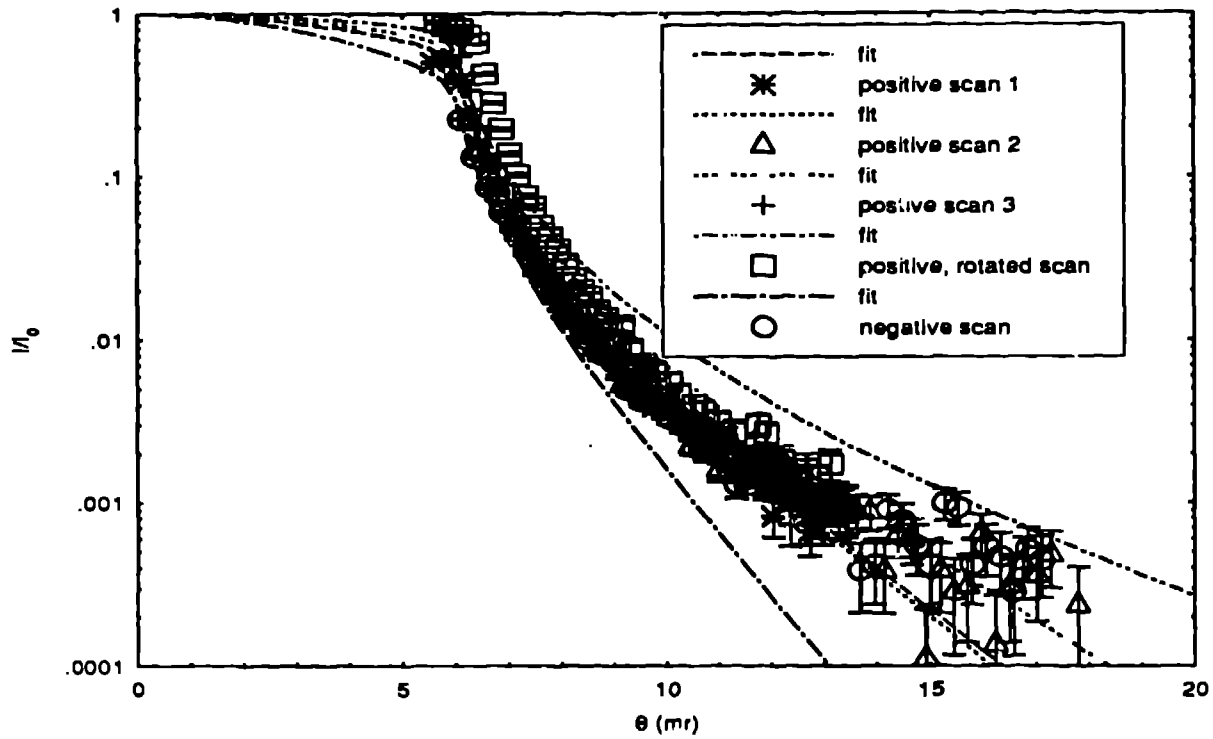
Single Crystal Molybdenum σ fits at 10keV

Figure 4: Single crystal molybdenum data and fits at 10 keV.
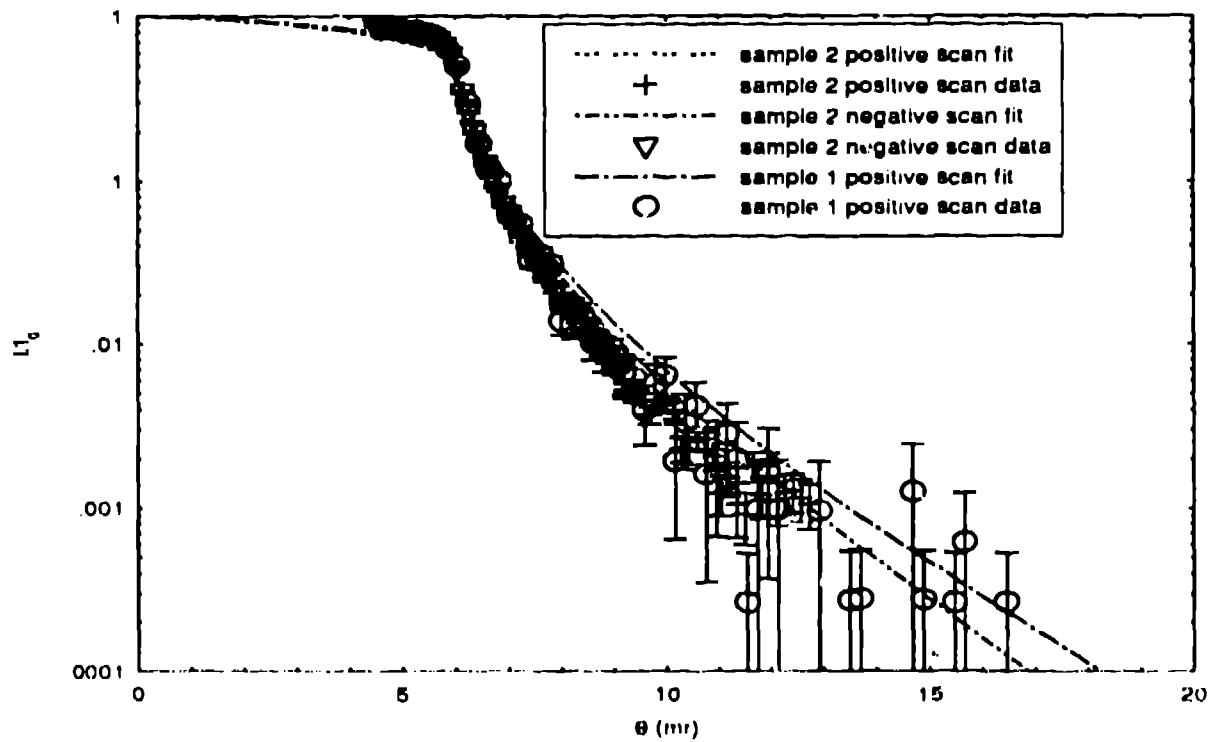
Polycrystalline Molybdenum σ fits at 10keV

Figure 5: Polycrystalline molybdenum data and fits at 10 keV.

Data showing the need for density determination are presented in Figure 6, which shows the 10 keV reflectivity

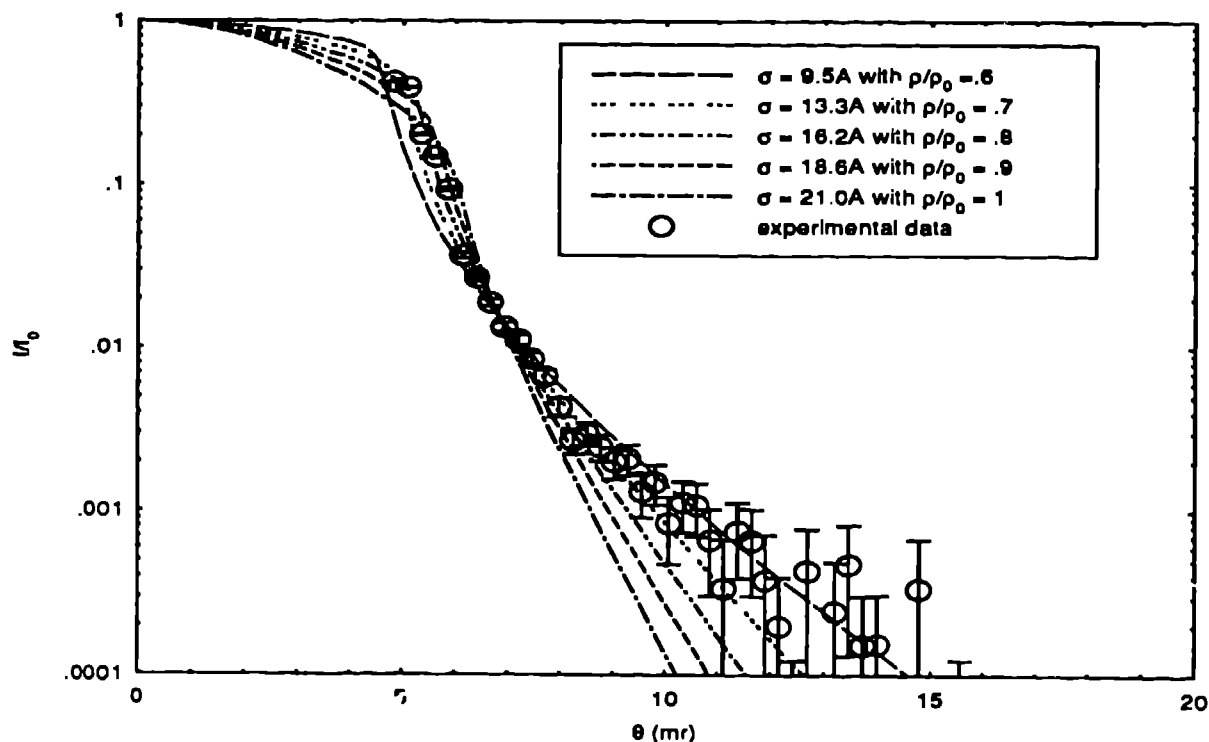**Evaporated Molybdenum Fits with Density Varied**

Figure 6: Evaporated molybdenum fit for σ with varying assumed densities ($\rho_0 = 10.4\,\mathrm{gm/cm^3}$)

of Mo evaporated onto a glass disc. Several assumed densities were used in the roughness model. Accurate fitting of the data in figure 6 required variation of both density and surface roughness.

A selection from numerous angle and energy scans on the low energy beamline U3C is shown in figure 2. The monochromator was scanned from 100 eV to 290 eV for the reflected beam. Then the scan was repeated with the single crystal Mo sample removed. Both scans of the NBS diode detector were normalized against the mesh monitor diode, which has a geometry identical to the NBS diode but with a 54% transmission mesh photocathode. Both detectors have a very low sensitivity of current out per X-Ray signal in. Consequently, the low reflectivity range $\approx 190 - 280\,\mathrm{eV}$ may have some systematic error from electrometer background. Also in this range there is lower energy stray light from the monochromator which causes a false excess of reflectivity. Any carbon contamination layer should have a negligible effect at this angle of incidence. No error estimates were included quantitatively yet. Other data, not shown here, at 64.5 mrad do show the dispersion dip from the Mo M_V edge around 245 eV, but cannot be used for the optical constants until they are remeasured with the stray light removed.

5 RESULTS

Roughness estimates were obtained at several energies including repeats. These show reasonable dispersion on repeat scans at a fixed energy and essentially the same values from 5 to 11 keV. Figure 7 shows the results of fitting all the measured curves. Roughness and density have similar effects on the fits to the evaporated samples as is seen in figure 6. A best fit was obtained for a density of 80 percent of the bulk density and surface roughness of 14.8 Å (RMS) The WYKO roughness was only half as large, 7.5 Å. This difference is disturbing since the bulk density samples exhibited good agreement between the WYKO and averaged fitted roughness values — these were respectively 9.5 Å and 9.3 Å for polycrystalline Mo, and 12.9 Å and 10.3 Å (RMS) for single crystal Mo. Similar discrepancies between WYKO and fitted reflectivity data on sputtered samples have been observed by Gullikson[5] and by Windt and Kortright.[19]
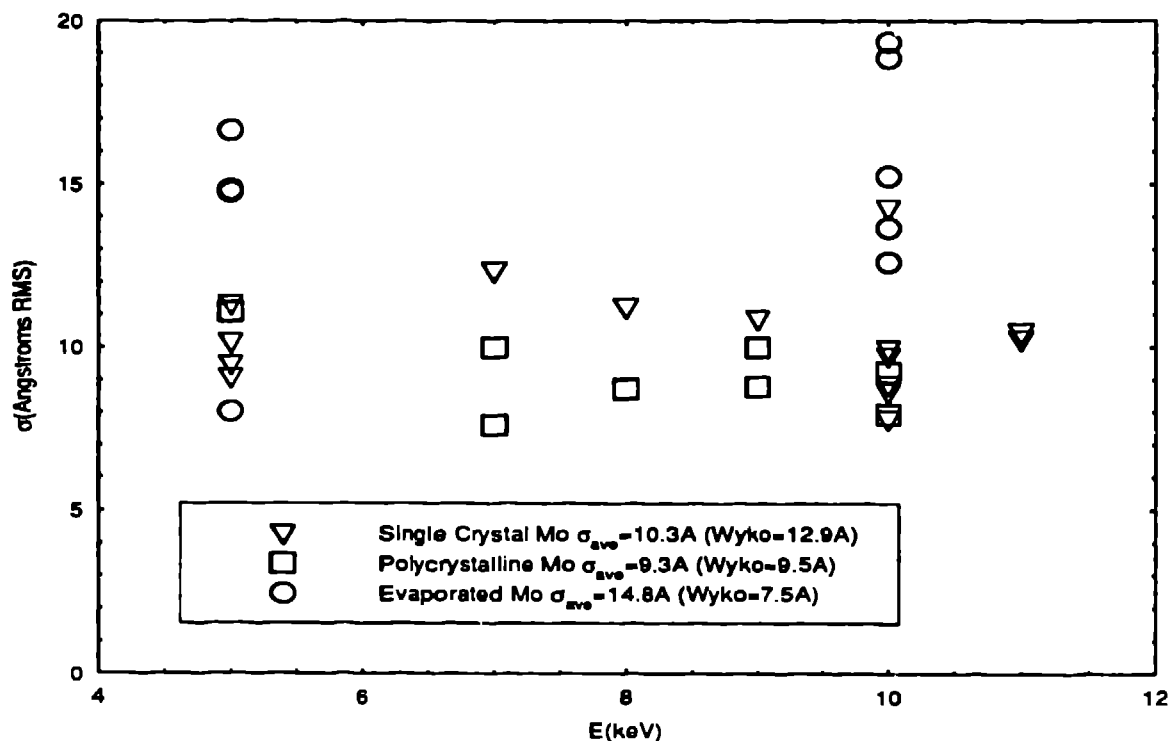
Figure 7: Molybdenum σ fitting results.

The low energy data on single crystal Mo reflectivity versus energy (figure 2) show that more than roughness is required for a fit, even to data contaminated with dark current and stray light. The portion of the data around the high energy cutoff ($\approx 150 - 180\,eV$) was modeled with material constants from Henke, et. al.[6] and the surface roughness 10.3 Å from the X8C measurements. To obtain any better fit we had to use an assumed density of 90 percent of bulk density. This arbitrary adjustment made good sense when one of us (JCD) realized that the Henke data[6] were based primarily on the measurements of Windt, et. al.[7] with an assumed bulk density of 10.4 gm/cm³, when in fact the data were measured on evaporated samples for which a lower density must have applied — 90 percent of bulk density in this case is quite reasonable. Therefore, we have a result showing the need for an approximately 10 percent upward revision of the absorption coefficient tables for Mo in the 100-300 eV range. We also confirm the need to determine the density of any evaporated or sputtered samples before accurate material constants may be extracted from the data.

6 FUTURE IMPROVEMENTS

Success in this program will require improvements in several areas. We shall just enumerate the ones that are obvious from these first measurements:

1. Sample surfaces must be flat to $\lambda/20$ or better and have roughness of 5 Å RMS or better. Scratches and dust should be masked and minimized respectively.

2. Sample mounts should be designed so the incident beam can never see the mount surface or edges.

3. Evaporated and sputtered samples need some independent measurements, such as Auger Electron Spectroscopy with ion etching, to establish the distribution and fraction of impurities with depth.

4 Contamination layers of carbon that form in intense synchrotron beams can be reduced by placing cold surfaces close to the optical elements and by rf-plasma cleaning. A high vacuum reflectometer will also be needed to control this contamination

5. Transfer chambers should be used between the high vacuum evaporator and reflectometer to minimize dust and contamination.

6. Scattered light and harmonics from synchrotron XUV monochromators must be reduced.

7. Detection and monitoring of the beam flux must be optimized for each synchrotron beamline. Monitoring must be accomplished downstream of the last slit before the sample.

8. X-Ray beamlines should be operated with a vacuum or helium beam path to avoid suppression of the monochromator first order relative to the higher energy harmonics.

9. Detection systems must be designed with low background and a dynamic range of 10^5 or better.

10. When using photon counters one must include deadtime corrections and design for high count rates.

11. At NSLS we must identify and eliminate the causes of signal oscillations and other systematic problems.

12. Slit quality is extremely important for measurements at glancing angles below 10 mrad.

13. Further work must be done to understand the differences between WYKO and fitted roughness for evaporated and sputtered samples.

7 CONCLUSIONS

The agreement between WYKO and fitted roughness parameters is good for single crystal and polycrystalline samples, but is poor for evaporated and sputtered samples. Possibly the impurities entrained in evaporated and sputtered samples change reflectivity curves in the tail enough to bias the fits.

Achievement of high accuracy on optical constant determinations from mirror reflectivity measurements will require measurements at both high and low energy with the utmost care to reduce systematic errors. Nevertheless, it should provide a valuable supplement to direct absorption measurements which yield β or f_2 alone.

Measurements at one or two energies between 5 and 10 keV should be adequate for angular scans of reflectivity to determine sample roughness. It is not clear how density and roughness can both be evaluated for sputtered and evaporated samples. Perhaps a two parameter fit over portions of the total curve will provide convergent results. To verify this we need better data in the high angle tails where the roughness parameter dominates.

"Calibrations science" generally places more stringent demands on source stability, purity, and monochromaticity than do some other sciences. This makes one's tasks especially difficult for absolute calibrations on XUV synchrotron beamlines.

8 ACKNOWLEDGMENTS

9 REFERENCES

[1] D. E. Graessle,, et. al., "Grazing incidence x-ray reflectivity: studies for the AXAF Observatory," *Proc. SPIE* **1546** (1991).

[2] M. F. Toney and S. Brennan, "Measurements of carbon thin films using x-ray reflectivity," *J. Appl. Phys.* **66**(4), pp. 1861 1863 (1989).

[3] L. A. Smirnov, T. D. Sotnikova, B. S. Anokhin, and B. Z. Taibin, "Total external reflection of x-rays from rough surfaces," *Opt. Spectrosc. (USSR)* 46(3), pp. 329-332 (1979).

[4] D. G. Stearns, "The scattering of x rays from nonideal multilayer structures," *J. Appl. Phys.*, 65 (2), pp. 491-506 (1989).

[5] E. M. Gullikson, *private comm.*

[6] B. L. Henke, J. C. Davis, E. M. Gullikson, and R. C. C. Perera, "A Preliminary Report on X-Ray Photoabsorption Coefficients and Atomic Scattering Factors for 92 Elements in the 10-10000 eV Region," *Lawrence Berkeley Laboratory report LBL-26259* (Nov. 1989).

[7] D. L. Windt, W. C. Cash, Jr., M. Scott, P. Arendt, B. Newnam, R. F. Fisher, and A. B. Swartzlander "Optical constants for thin films of Ti, Zr, Nb, Mo, Ru, Rh, Pd, Ag, Hf, Ta, W, Re, Ir, Os, Pt, and Au from 24 Å to 1216 Å," *Appl. Opt.*, 27 (2), pp. 246-278 (1988).

[8] D. L. Windt, W. C. Cash, Jr., M. Scott, P. Arendt, B. Newnam, R. F. Fisher, A. B. Swartzlander, P. Z. Takacs, and J. M. Pinneo, "Optical constants for thin films of C, diamond, Al, Si, and CVD SiC from 24 Å to 1216 Å," *Appl. Opt.*, 27 (2), pp. 279-295 (1988).

[9] R. L. Blake and T. Passin, "X-Ray Astronomy Laboratory at the University of Chicago," *Advances in X-Ray Analysis*, C. S. Barrett, J. B. Newkirk, and C. Rudd, Eds., Vol. 14, pp. 293-310, Plenum Press, New York (1970).

[10] R. J. Bartlett, W. J. Trela, F. D. Michaud, S. H. Southworth, R. W. Alkire, P. Roy, R. Rothe, P. J. Walsh, and N. Shinn, "Characteristics and Performance of the Los Alamos VUV beamline at the NSLS," *NIM A* 266, pp. 199-204 (1988).

[11] W. J. Trela, R. J. Bartlett, F. D. Michaud, and R. Alkire, "An X-Ray Beam Line for the Energy Range 5-20 keV," *NIM A* 266, pp. 234-237 (1988).

[12] E. D. Palik, Ed., *Handbook of Optical Constants of Solids*, Academic Press, Orlando (1985).

[13] J. H. Weaver, C. Krafka, D. W. Lynch, E. E. Koch, "Optical Properties of Metals," *Physik Daten, Physics Data*, Vol. 18-1, Vol. 18-2, Fach-information Zentrum, Karlsruhe (1981).

[14] R. L. Blake, B. Davis, J. C. Davis, D. E. Graessle, R. Hockaday, D. Holmberg, "The Los Alamos high throughput XUV beamline at NSLS," *in prep.*

[15] W. L. Bond, "Precision Lattice Constant Determination,", *ACTA Crystallogr.* 13, pp. 814-818 (1960).

[16] R. L. Blake, "Plane Crystal Measurements in the Ultrasoft X-Ray Region with Application to solar Physics," *NCAR Cooperative Thesis No. 15*, Univ. of Colorado and High Altitude Observatory, (1968).

[17] J. L. Thompson, "High Precision X-Ray Spectroscopy," in *X-Ray Spectroscopy*, ed. L. Z. Azároff, McGraw-Hill, New York, pp. 26-132 (1974).

[18] W. H. Press, B. P. Flannery, S. A. Teukolsky, and W. T. Vetterling, *Numerical Recipes*, Ch. 14, Cambridge University Press, Cambridge, (1986).

[19] D. L. Windt and J. B. Kortright, "XUV Optical Characterization of Thin Film and Multilayer Reflectors," *Proc. SPIE*, 1160, pp. 246-258 (1989).

DISCLAIMER